New Journal of Physics
The open-access journal for physics

Fault-tolerant computing with biased-noise superconducting qubits: a case study

P Aliferis[1,3,4], F Brito[1,3], D P DiVincenzo[1,4], J Preskill[2], M Steffen[1] and B M Terhal[1]

[1] IBM Watson Research Center, Yorktown Heights, NY 10598, USA
[2] Institute for Quantum Information, California Institute of Technology, CA 91125, USA
E-mail: panos@alumni.caltech.edu and divince@watson.ibm.com

New Journal of Physics **11** (2009) 013061 (19pp)
Received 23 September 2008
Published 30 January 2009
Online at http://www.njp.org/
doi:10.1088/1367-2630/11/1/013061

Abstract. We present a universal scheme of pulsed operations suitable for the IBM oscillator-stabilized flux qubit comprising the controlled-σ_z (CPHASE) gate, single-qubit preparations and measurements. Based on numerical simulations, we argue that the error rates for these operations can be as low as about 0.5% and that noise is highly biased, with phase errors being stronger than all other types of errors by a factor of nearly 10^3. In contrast, the design of a controlled-σ_x (CNOT) gate for this system with an error rate of less than about 1.2% seems extremely challenging. We propose a special encoding that exploits the noise bias allowing us to implement a *logical* CNOT gate where phase errors and all other types of errors have nearly balanced rates of about 0.4%. Our results illustrate how the design of an encoding scheme can be adjusted and optimized according to the available physical operations and the particular noise characteristics of experimental devices.

After years of painstaking labor, superconducting qubits [1] are taking shape as viable elements for the construction of a scalable quantum computer. Since the initial demonstration of coherent quantum dynamics in superconducting qubits [2]–[5], it has been recognized that these systems have great potential versatility [6]–[8], so that one can genuinely envision a quantum-computing integrated circuit emerging from this research. However, no clear way forward has been announced, owing largely to one undeniable feature of large-scale quantum computation: it

[3] Contributed equally to this work.
[4] Authors to whom any correspondence should be addressed.

will require a very high degree of fidelity in the execution of quantum operations, much higher than has been reported in any present experiments.

How high a fidelity, or how low an error rate, will be needed? On the basis of fundamental early theoretical work [9]–[11], lip service is frequently paid to a necessary universal set of operations containing the two-qubit controlled-σ_x (CNOT) gate, and a necessary 'threshold' error rate in the 10^{-5}–10^{-4} range. Some recent modeling for superconducting qubits [12, 13] suggests that such noise levels could conceivably be reached in the lab; however, in current experimental practice the ability even to reliably *detect* such small error rates, let alone to achieve them, is in fact very questionable.

In this paper, we will consider the possibility of constructing a universal set of operations for the IBM 'Koch qubit' [8, 14][5]. Although our set of operations will not contain the CNOT gate, we will propose an encoding scheme for implementing *logical* CNOT gates which can then be used for fault-tolerant quantum computation. With the combination of our encoding scheme and other improvements in the theory of quantum fault tolerance [15]–[17], error rates for our elementary operations in the 0.1–0.5% range are expected to be tolerable for practical quantum computation. We estimate using numerical simulations that error rates in this range are possible for the Koch qubit. Though these estimates are far from the error rates that have been currently measured in experiments, we hope our results will motivate and stimulate the research in superconducting qubits in the IBM lab and elsewhere. More generally and even beyond superconducting qubits, our encoding scheme illustrates how techniques of quantum error correction and fault tolerance can be tailored to the available physical operations and the particular noise characteristics of experimental devices.

Our proposal involves a synthesis of recent experimental and theoretical developments. On the experimental side [8, 14], pulsed operations for the Koch qubit were discussed in [18]; the set of operations considered in [18] included the controlled-σ_z (CPHASE) gate, the Hadamard (H) gate, single-qubit 'diagonal' rotations of the form $\exp(\mathrm{i}\theta\sigma_z)$, the preparation of a qubit in the state $|+\rangle = \frac{1}{\sqrt{2}}(|0\rangle + |1\rangle)$ and the measurement of σ_x (where σ_x, σ_y and σ_z are the Pauli spin operators). For these operations [18] numerically estimated the error rates by considering all physical sources of noise that we presently know how to model for this system—$1/f$ flux noise, instrumental jitter in pulse timing and amplitude, and Johnson noise from resistances in the circuit. For the CPHASE gate it estimated an error rate of about 0.45%, for the H gate about 0.4%, for diagonal rotations about 0.001% for any θ, for the preparation of the state $|+\rangle$ about 0.3% and for the measurement of σ_x about 0.2%.[6]

In contrast, no direct implementation of a CNOT gate with error rate close to even 5% could be devised for the Koch qubit. Alternatively, a CNOT gate can be implemented indirectly by composing other elementary operations. Figure 1 shows two possible methods: the first indirect implementation uses one CPHASE and two H gates, whereas the second one uses three CPHASE gates, two qubits prepared in the state $|+\rangle$, and two measurements of σ_x. Therefore, we estimate that the first indirect implementation would have an error rate of about 1.25%, and the second one about 2.3%.

Based on the modeling in [18], it was further observed that noise in the CPHASE gate acted predominantly as dephasing; i.e. it affected the relative *phases* in the wavefunction giving rise to

[5] After Roger Hilsen Koch (1950–2007), the leader of the experimental superconducting-qubit effort at IBM Research until his sudden death on 4 August, 2007.

[6] These numbers are obtained by using the results in [18] and the definition of an error rate in the appendix. In [18], the entanglement fidelity and not the error rate is used as a measure of the noise strength.

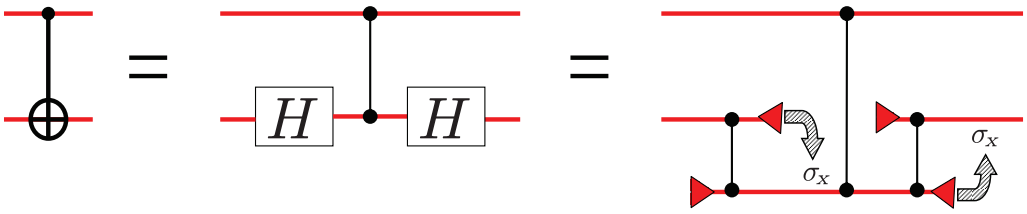

Figure 1. On the left, a CNOT gate is applied between two qubits. In the middle, the CNOT gate is simulated by using one CPHASE and two H gates. On the right, another simulation where the two H gates are implemented by 'teleportation' using ancilla qubits and measurements. Vertical lines with dots on both ends denote CPHASE gates. A triangle pointing to the right denotes the preparation of a qubit in the state $|+\rangle$. A triangle pointing to the left denotes a measurement of σ_x. Conditioned on the measurement outcomes, σ_x correction operators may be necessary as shown.

'phase' errors, which can be expressed as diagonal matrices in the computational basis. All other errors, including errors due to relaxation and also 'leakage' errors associated with transitions to states outside the computational space, were observed to be about an order of magnitude weaker. The same observation also applies to single-qubit diagonal rotations but, on the other hand, no similar bias was observed for the noise in the H gate.

On the theoretical side, the findings of [18] motivated us to revisit a longstanding problem in the theory of fault-tolerant quantum computation: how to formulate an encoding scheme that exploits large asymmetries in the *structure* of noise in elementary operations. Here and in our companion paper [19], we present such a scheme based on encoding the noisy qubits using a repetition code, and we show how fault-tolerant *logical* CNOT gates can be implemented for this code. The intuition we gained from [18] is that highly biased noise, with phase errors being much stronger than all other types of errors, is possible for gates such as the CPHASE, but it should not be physically expected for generic operations. Furthermore, an encoding scheme has to address the problem that a noise bias can easily be lost as elementary operations are composed together.

Our solution is to choose a universal set of elementary operations whose implementation induces noise that is biased towards dephasing, and where all gates commute with σ_z so that the noise bias is maintained. The operations we will use are the preparation of the state $|+\rangle$, the controlled-σ_z (CPHASE) gate and measurements of observables in the equator of the Bloch sphere, i.e. of the form $\exp(\mathrm{i}\theta\sigma_z)\sigma_x$ for certain angles[7]. Noise for the preparation of the state $|+\rangle$ is naturally biased since $|+\rangle$ is an eigenstate of σ_x. The structure of noise for the CPHASE gate depends on the physical implementation and it can be engineered to be biased; here, we propose such a biased-noise implementation for the Koch qubit based on *adiabatic* pulses so that transitions between the computational-basis states are strongly suppressed. Finally, noise in

[7] Alternatively, we may restrict to measurements of σ_x, if we add to our set of elementary operations the preparation of the states $|+i\rangle = \exp(\mathrm{i}(\pi/4)\sigma_z)|+\rangle$ and $|T\rangle = \exp(\mathrm{i}(\pi/8)\sigma_z)|+\rangle$; this is the universal set considered in [19]. For the Koch qubit, it is more natural to move all rotations of the form $\exp(\mathrm{i}\theta\sigma_z)$ before the measurements since, as we will discuss, corrective single-qubit diagonal rotations are necessary in the implementation of every CPHASE gate.

a single-qubit measurement can be described by errors preceding the ideal measurement which need not have any specific structure since measurement has a classical output.

These theoretical ideas should be relevant both for the experiments with the Koch qubit and for solid-state qubits in general. They suggest that a profitable focus of experiments could be to design qubits with long relaxation time T_1. Provided this is achieved, dephasing, which is the dominant source of noise, can be much more effectively suppressed by using our encoding scheme. Furthermore, the implementation of low-noise CNOT or H gates is not necessary; it suffices to implement CPHASE gates with highly biased noise, together with single-qubit preparations and measurements. For the Koch qubit, eliminating the need to implement the H gate allows us to re-examine the pulse schemes in [18], and to find a simpler implementation of the CPHASE gate for which noise is much more biased than in [18]. Similar simplifications may be possible in other types of superconducting qubits. In particular, a standard experimental approach to suppressing dephasing noise is to intersperse quantum gates with additional corrective 'hardware' operations such as spin echo pulses. Our encoding scheme can be seen as a complementary solution where the hardware operations are restricted to a much smaller set and dephasing is suppressed at the 'software' level by using error correction applied on blocks of several noisy qubits.

We will now discuss the details of our proposal. The central question is how to devise a strategy for fault-tolerant quantum computation that effectively exploits a bias in the noise of the CPHASE gate. To develop some intuition, let us assume for the moment that there is no leakage, that independent phase errors occur with probability ε, and that all other types of errors occur with probability $\varepsilon' \ll \varepsilon$. Then a clear strategy for the lowest-level coding of quantum data is to use an n-qubit repetition code. One logical qubit is encoded in a 'block' of n physical qubits, a logical $|+\rangle$ state is represented by all n qubits being in the state $|+\rangle$, and a logical $|-\rangle$ by all n qubits being in the state $|-\rangle$. Since the logical σ_z operator is a σ_z acting on all n qubits in the block, phase errors on more than half of the qubits in the block are necessary for a logical error to occur after error correction; taking n odd, and assuming that for each qubit there are t time steps where a phase error may occur, the probability of a logical error is approximately

$$\varepsilon_{\mathrm{L}} \approx \binom{n}{\frac{n+1}{2}} (t\varepsilon)^{(n+1/2)}. \tag{1}$$

On the other hand, the logical σ_x operator is a σ_x acting on *any* qubit in the block, so that even a single error different from a phase error on any qubit and at any time step cannot be corrected; thus, the probability of a logical error is approximately

$$\varepsilon'_{\mathrm{L}} \approx nt\varepsilon'. \tag{2}$$

If the noise 'bias' ε/ε' is large, we can choose some large n and obtain a significant reduction of the *logical* error rate; e.g. if the bias is 10^3 and even for $t \cdot \varepsilon = 5\%$, we find that $\varepsilon_{\mathrm{L}} \approx \varepsilon'_{\mathrm{L}} < 3.5 \times 10^{-4}$ by setting $n = 7$. This sends an optimistic message, since several schemes are known for effectively implementing fault-tolerant quantum computation with error rates of order 10^{-4} [20].

As we will discuss below, our pulsed implementation of a CPHASE gate can in fact be optimized to lead to a noise bias of order 10^3. But first, we must examine more closely whether there is actually a gain in using the repetition code as our naive argument so far indicates. The main concern is that a large intrinsic noise asymmetry in our elementary operations might be spoiled as these operations are composed together.

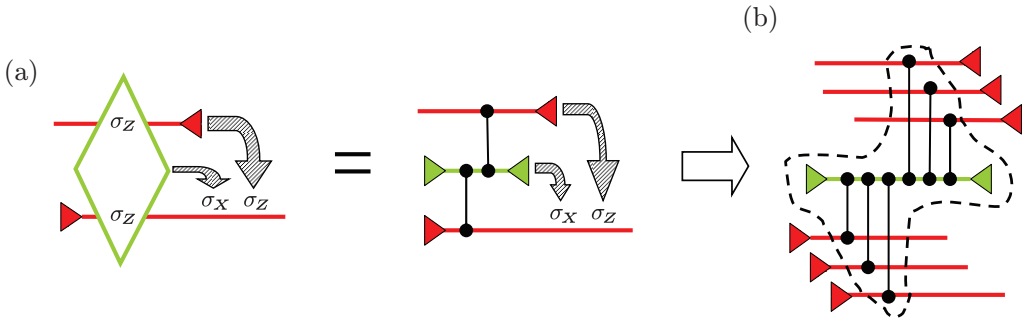

Figure 2. (a) On the left, an identity circuit which consists of preparing a qubit in the state $|+\rangle$, measuring $\sigma_z \otimes \sigma_z$ on this qubit and the input qubit, and finally measuring σ_x on the input qubit. After applying the correction operators shown conditioned on the measurement outcomes, the state of the input qubit is 'teleported' to the output qubit. On the right, the measurement of $\sigma_z \otimes \sigma_z$ is implemented by using an 'ancilla' qubit (shown in green) which interacts with the other two 'data' qubits (shown in red) via CPHASE gates before it is measured. (b) The circuit in (a) where the data qubits are encoded in the n-bit repetition code (here $n = 3$); the ancilla qubit remains unencoded, but the subcircuit enclosed by the dashed curve must be repeated sequentially several times, and the majority of the measurement outcomes must be taken in order to correct errors (the repetitions are not shown). As in (a), logical σ_z or σ_x correction operators (not shown) may be necessary on the output data block.

For example, consider the problem of implementing a logical CNOT gate between two blocks of encoded qubits. The logical CNOT gate for the repetition code can be implemented by bitwise CNOT gates, and each CNOT gate can be simulated by using CPHASE gates as in figure 1. But then due to the H gates, phase errors that occur during the simulation of each CNOT gate are converted into errors of other types; e.g. a σ_z error during the implementation of a H gate will be converted to some linear combination of a σ_z, a σ_x and a σ_y error. So, this construction of a logical CNOT gate destroys the asymmetric structure of the noise and nullifies the effectiveness of the repetition code. Avoiding this interconversion of noise is possible, but it requires a circuit of greater complexity. At the heart of this circuit construction is the identity operation in figure 2(a); it consists of preparing a qubit in the state $|+\rangle$, measuring $\sigma_z \otimes \sigma_z$ on this qubit and the input qubit, and finally measuring σ_x on the input qubit.

The basic idea is now to encode the qubits in the repetition code. We have already mentioned that the preparation of a logical $|+\rangle$ involves simply preparing every qubit in the block in the state $|+\rangle$. A measurement of the logical σ_x is also very simple and robust; it can be implemented by measuring σ_x on each qubit in the block, and then taking the majority of the outcomes to correct errors. It remains to discuss how to implement a measurement of the logical $\sigma_z \otimes \sigma_z$ on the two blocks. The difficulty is that the measurement must be robust against the dominant phase errors, and it must also respect the biased structure of the noise. Figure 2(b) shows our solution: a single unencoded 'ancilla' qubit is prepared in the state $|+\rangle$, and then CPHASE gates are applied between this ancilla qubit and all other qubits in the two blocks. Finally, a measurement of σ_x is performed on the ancilla, and a logical σ_x correction may be necessary on the output block conditioned on the measurement outcome. Since even a single

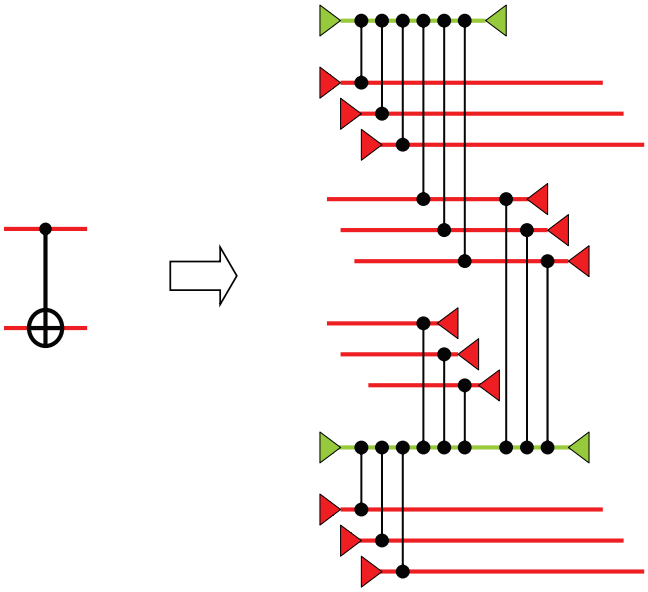

Figure 3. A logical CNOT gate between two blocks encoded in the repetition code (here again, the 3-bit code). Ancilla qubits (shown in green) are prepared in the state $|+\rangle$, they interact via CPHASE gates with the data qubits (shown in red), and they are measured along the eigenbasis of σ_x. As in figure 2, the measurements with ancilla qubits must be repeated sequentially several times so that errors can be corrected by taking the majority of the outcomes (the repetitions are not shown). Finally, σ_x is measured on each qubit in the two input blocks, and the majority is taken on each block. Conditioned on the results of the majorities, logical correction operators (not shown) may be necessary on the output blocks [19].

phase error on the ancilla can cause an error in the measurement outcome, the measurement of the logical $\sigma_z \otimes \sigma_z$ must be repeated sequentially several times; by taking the majority of the outcomes we can suppress the probability of a logical error at the output.

Using the building blocks just discussed, it is possible to construct a fault-tolerant logical CNOT gate that respects the physical-level bias of the noise; see figure 3. This circuit implements a logical CNOT gate between the two blocks encoded in the repetition code, while at the same time the logical state of each block is teleported to a new block and phase errors are corrected. Because of the use of teleportation, this circuit has the additional feature that it largely prevents the propagation of leakage errors. In figure 3, the output data qubits always interact with an ancilla qubit prior to any interaction with the input data qubits; therefore, there is no possibility for leakage to propagate from the input to the output qubits. And furthermore, if we consider implementing a sequence of logical CNOT gates, we observe that every qubit is eventually measured after only a small, fixed number of time steps, and the measurement effectively converts leakage to regular qubit errors [21].

In addition, it is possible to construct with the same building blocks a fault-tolerant preparation of the logical $|0\rangle$ and $|+\rangle$ states, and a measurement of the logical σ_z and σ_x for the repetition code. The logical CNOT gate, the preparation of logical $|0\rangle$ and $|+\rangle$, the measurement of logical σ_z and σ_x, and single-qubit measurements of $\exp(i\theta\sigma_z)\sigma_x$ for $\theta = \pi/4$ and $\pi/8$ suffice

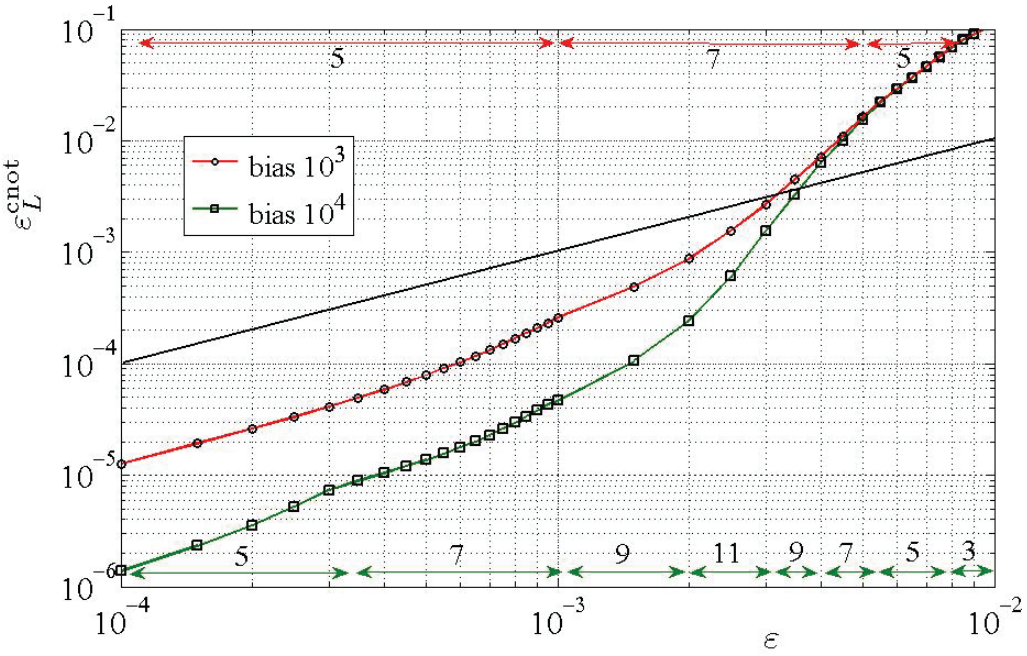

Figure 4. Upper bounds on the total probability $\varepsilon_{\mathrm{L}}^{\mathrm{cnot}}$ of logical errors for the logical CNOT gate as a function of the probability ε of physical-level phase errors for a bias of 10^3 and 10^4. To obtain our bounds, we have optimized over the block size n of the repetition code, and the number k of repetitions of measurements with ancilla qubits; the optimal choice is to have $n = k$, while the optimal value depends on ε and the bias as shown. The straight line with slope unity serves as a guide to the eye.

for implementing universal fault-tolerant quantum computation; the full scheme is discussed in our companion paper [19].

Since our building blocks only use CPHASE gates, $|+\rangle$ preparations and σ_x measurements, and since phase errors commute with CPHASE gates, it is simple to estimate the error rates for the logical CNOT gate given the physical-level error rates. In [19], we give upper bounds for the logical error rates in closed form as a function of the block size n of the repetition code and the number k of repetitions of the measurements executed with ancilla qubits. The outcome is qualitatively as in equations (1) and (2) with $t = c\,k$ for some constant $c \approx 2$ or 3. It follows from this analysis that if the noise bias in our elementary operations is about 10^3 or greater, encoding in the repetition code is effective and logical errors are significantly weaker than the physical-level phase errors for ε of order 0.1% or smaller; see figure 4.[8]

The noise bias reported in [18] was about a factor of 10, which has motivated us to re-examine whether greater levels of bias are conceivable for the Koch qubit. As we will now discuss, the noise bias can, in fact, be dramatically improved at the expense of a very minor increase in the rate of phase errors. Figure 5 shows the structure of the Koch qubit [8, 14]. It is nominally a 'flux' qubit, meaning that the computational basis states $|0\rangle$ and $|1\rangle$ are quantum states corresponding to distinct circulating-current orientations; see figure 5. The mode

[8] Aliferis and Preskill [19] also discuss a more sophisticated procedure for decoding the repetition code which is effective for ε of about 0.5% or smaller. For simplicity, we do not analyze this decoding procedure in this paper.

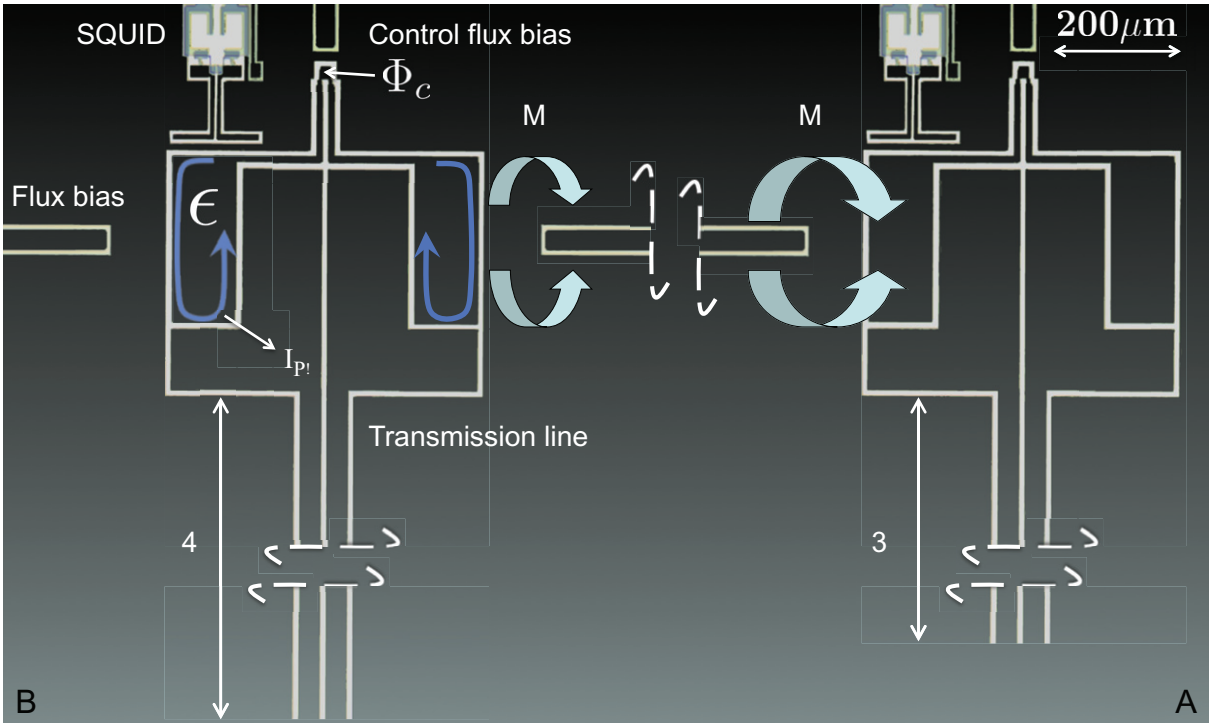

Figure 5. Physical layout of two Koch qubits [8] coupled as needed to implement a CPHASE gate. Qubits A and B differ only in the resonant frequencies of the transmission line resonators attached to them. These frequencies are controlled by the physical length of the transmission lines, and are in the ratio 3 : 4. The single-qubit device Hamiltonians can be varied independently by controlling the 'control flux' Φ_C corresponding to the flux through the small loop, and the 'flux bias' ϵ corresponding to the flux difference in the two large loops. The SQUIDs perform quantum measurements on the states of the individual qubits. The qubits are coupled via a fixed mutual inductance M to a superconducting loop. For small values of Φ_C, the basis states $|0\rangle$ and $|1\rangle$ of each qubit correspond to different orientations, counterclockwise and clockwise, of the persistent current I_P.

of operation is highly tunable via an external 'control flux' Φ_C threading the small loop; see figure 6. At small Φ_C, the degeneracy of the two circulating-current states is lifted by the 'flux bias' ϵ corresponding to the flux difference in the two large loops, and the two basis states are easily detected and initialized but not very phase coherent. As Φ_C is increased, the barrier decreases until it eventually disappears, and tunnel splitting between the basis states turns on rapidly. At even larger Φ_C, we enter an almost harmonic single-well regime, but before this another essential element of the Koch qubit enters the picture.

The flux-qubit states are strongly coupled to the fundamental mode of a superconducting transmission-line resonator, so that $|0\rangle$ and $|1\rangle$ pass via an avoided level crossing to $|\tilde{0}\rangle$ and $|\tilde{1}\rangle$ corresponding to the 0- and 1-photon modes of the oscillator. The superconducting transmission line is highly phase coherent [8]. In the IBM experiments we have seen about 50 000 Ramsey fringes associated with these states corresponding to $T_2 = 2.5\,\mu$s [22]; we expect much longer T_2 times to be possible. This fact has led us in [18] to the following strategy for implementing

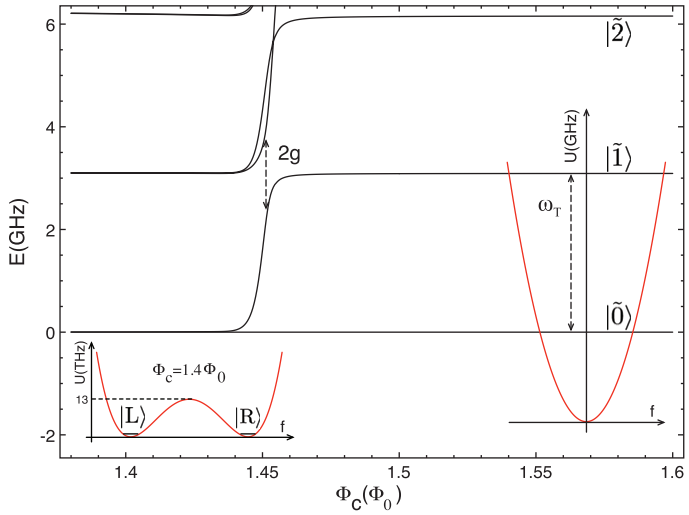

Figure 6. The lowest energy levels of a single Koch qubit on the 'symmetric line' corresponding to $\epsilon = 0$, as a function of Φ_C. For small Φ_C, $\Phi_C = 1.4\Phi_0$ ($\Phi_0 = h/2e$), the ground state is doubly degenerate; the degeneracy may be lifted by setting $\epsilon \neq 0$, allowing for qubit measurement and preparation. The two basis states $|0\rangle$ and $|1\rangle$ correspond to the two states $|L\rangle$ and $|R\rangle$ of a double-well potential with a very large potential barrier between them as sketched, which describe the two different orientations of the persistent current I_P in the flux qubit; the rescaled dynamical variable f is explained in [23]. For both $|0\rangle$ and $|1\rangle$, the superconducting transmission line is in its 'vacuum' 0-photon state. As Φ_C is increased to around $1.45\Phi_0$, the barrier height drops, leading to a rapid increase in the tunnel splitting between the two lowest states. When the tunnel splitting equals the transmission-line resonator frequency ω_T, there is an avoided level crossing with splitting $2g$. For larger Φ_C, the qubit is 'parked'; now, the two lowest energy states $|\tilde{0}\rangle$ and $|\tilde{1}\rangle$ correspond to the 0- and 1-photon states of the transmission line, respectively, their energies are independent of Φ_C, and their effective potential is highly harmonic as sketched. In this regime, for both $|\tilde{0}\rangle$ and $|\tilde{1}\rangle$, the flux-qubit state is the symmetric state $|S\rangle \equiv \frac{1}{\sqrt{2}}(|L\rangle + |R\rangle)$.

low-noise operations. When not being acted upon, quantum information is stored in the highly coherent oscillator energy levels; we then say that the qubit is 'parked.' All needed operations are done by *adiabatic* pulsing out of parking. Each flux qubit has a fixed, untuneable two-qubit coupling to a set of nearby flux qubits in order to implement two-qubit gates. To assure that the effective coupling between parked qubits is negligible, these couplings are to be only between qubits with *different* resonator frequencies, so that resonant transfer of photons between different resonators does not take place in the parked state. Below we examine the simplest scheme with just two resonator frequencies, 3.1 and $\frac{3}{4} \times 3.1$ GHz (the commensurability of these frequencies aids in the maintenance of rotating frames for these qubits). Correspondingly, we have two species of qubits, A and B, respectively, and two-qubit couplings exist only between qubits of different species—this is not a severe restriction since, in our encoding scheme, the only interactions are between data qubits (red qubits in the figures) and ancilla qubits (green qubits).

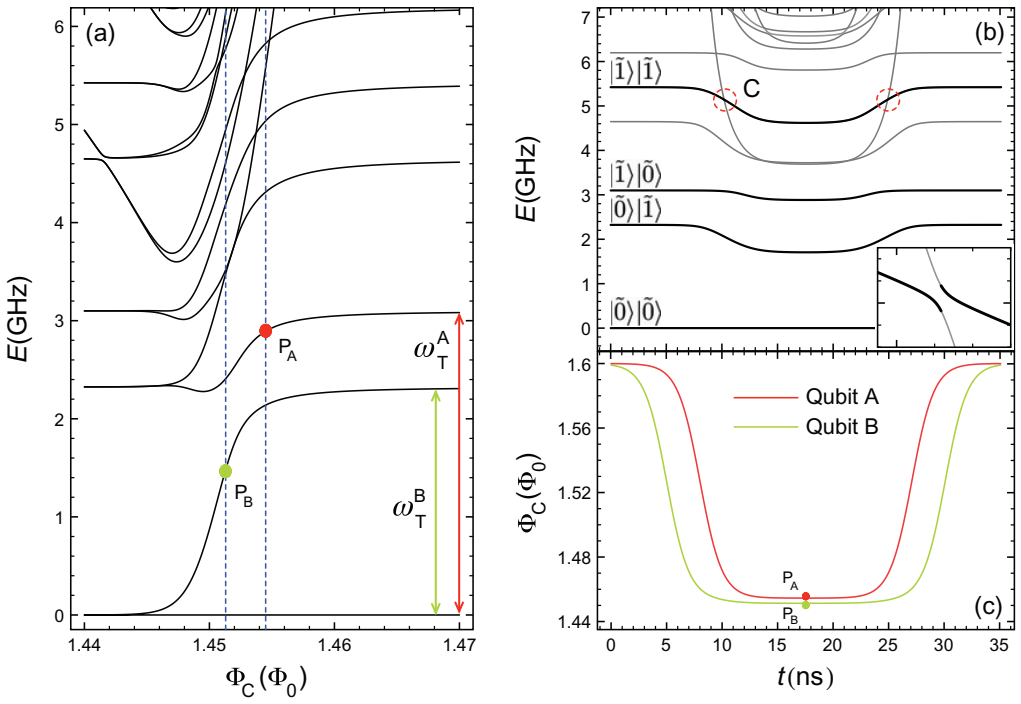

Figure 7. CPHASE gate modeling. (a) The energy levels of two coupled qubits for the special case $\Phi_C^A = \Phi_C^B$. (b) Variations of the eigenlevels of the two-qubit system for the optimal implementation of a CPHASE gate. To very good approximation, the quantum evolution adiabatically follows the four states $|\tilde{0}\rangle|\tilde{0}\rangle$, $|\tilde{0}\rangle|\tilde{1}\rangle$, $|\tilde{1}\rangle|\tilde{0}\rangle$ and $|\tilde{1}\rangle|\tilde{1}\rangle$. A crucial moment in the evolution is at the crossing C (and its time-reversed image in the second half of the pulse), when $|\tilde{1}\rangle|\tilde{1}\rangle$ crosses a state outside the computational space. Leakage to this state is suppressed because the avoided-crossing gap is very small (the inset shows the dispersion at C magnified by 200 000×), and because the angle of crossing is made larger by delaying the onset of the A pulse relative to the B pulse. Apart from this state and the four computational-basis states, all other eigenstates can be entirely left out of our numerical modeling because of their large distance from the $|\tilde{1}\rangle|\tilde{1}\rangle$ and $|\tilde{1}\rangle|\tilde{0}\rangle$ states. (c) The optimal control-flux pulses for A and B. Pulses are constructed as sums of tanh functions in order to have a standard smooth shape. It is found preferable to unpark A much less deeply (to P_a) than B (to P_b). Although P_a and P_b in (a) do not exactly correspond to the points P_a and P_b in (c) because Φ_C^A and Φ_C^B are not equal throughout the optimal pulses, they provide a good illustration of the relatively large energy difference (~ 1.5 GHz) corresponding to the small change in Φ_C ($\sim 0.004\Phi_0$) between P_a and P_b in (c).

Figure 7(a) shows the energy levels of the coupled two-qubit system as a function of the control flux—assumed equal for the two qubits in the figure—with the flux bias held on the 'symmetric line' $\epsilon = 0$ on which the effective qubit potential U has reflection symmetry as in figure 6. In the 'parking' region $\Phi_C \geqslant 1.46\Phi_0$, the effective interaction between the two qubits is strongly suppressed. The energy levels are essentially those of the unperturbed transmission line resonators and, because to very high accuracy we have energy additivity

$E(|\tilde{1}\rangle|\tilde{1}\rangle) = E(|\tilde{0}\rangle|\tilde{1}\rangle) + E(|\tilde{1}\rangle|\tilde{0}\rangle)$, there is no conditional phase accumulation in the two-qubit state. Out of parking, this energy additivity is violated and a *conditional* phase shift can accumulate. If only one qubit is pulsed out of parking, single-qubit 'diagonal' rotations of the form $\exp(-i\theta\sigma_z)$ can be effected (in the frame of reference rotating at the resonator frequency). If two coupled qubits are pulsed out of parking, a CPHASE gate can be implemented by choosing the pulse timing appropriately; at the same time, *known* single-qubit phase shifts accumulate which can be compensated by corrective diagonal rotations on each qubit [18].

There is, however, one point of concern which reveals itself more clearly when we plot the energy levels of the same two-qubit system as a function of time during the implementation of a CPHASE gate; see figure 7(b). At the energy-level crossing marked C, the avoided-crossing gap between the state $|\tilde{1}\rangle|\tilde{1}\rangle$ and a state *outside* the computational space becomes small, and this may potentially lead to increased leakage errors. One possible strategy to avoid this problem would be to increase the avoided-crossing gap by changing the flux bias to $\epsilon \neq 0$ in order to move away from the symmetric line; this solution was adopted in [18]. However, departing from the symmetric line has its disadvantages. The lowering of symmetry makes the system less protected from low-frequency noise, and it also causes the effective relaxation time T_1 to be shortened making it harder to achieve a high bias in the noise.

It would therefore be desirable to perform the operation at the symmetric line. Our new observation is that the avoided-crossing gap is actually very small; it is never larger than 100 kHz even taking parameter shifts due to low-frequency noise into account. So for our pulse profiles, the Landau–Zener tunneling probability is extremely close to one, meaning that we can pulse through the avoided-crossing gap and suffer essentially no leakage. After trying many pulse designs, and checking the noise bias they produce, we find the pair of pulses in figure 7(c) for the two species of qubits to work the best. We observe that in this pulsing scheme the low-frequency qubit B is unparked far more deeply (point P_b) than the high-frequency qubit A (point P_a); this choice is optimal because, if the two species of qubits were unparked symmetrically, the same level of dephasing noise could only be maintained by making the pulse duration significantly longer increasing the noise due to relaxation and leakage.

To estimate the effect of noise in the implementation of our CPHASE gate, we have performed multiple computer simulations of the evolution of the two coupled qubits during the gate where, in each simulation, low-frequency noise is added to the ideal dynamics. To model low-frequency noise, in each simulation we take the actual applied flux and the actual timing in a pulse to deviate from the ideal by an amount which is chosen from a Gaussian distribution with zero mean and variance $6\mu\Phi_0$ and 6 ps, respectively [18]. From each simulation we extract a unitary which describes the noisy implementation of the CPHASE gate; by averaging over a large number of simulations which corresponds to integrating over the Gaussian fluctuations, we obtain a superoperator describing the noisy implementation of the gate. By expressing this superoperator as $\mathcal{N} \circ \mathcal{CZ}$ where $\mathcal{CZ}$ is the ideal superoperator when there is no noise, we can define an 'error rate' in terms of the norm of $\mathcal{E} = \mathcal{N} - \hat{\mathcal{I}}$ where $\hat{\mathcal{I}}$ is a trace-decreasing superoperator proportional to the identity superoperator. Although this rate does not necessarily correspond to the probability of an error, it is possible to formulate a fault-tolerance analysis similar to the case of stochastic noise. In particular, we may expand $\mathcal{E} = \mathcal{E}_{\text{phase}} + \mathcal{E}_{\text{other}}$, where $\mathcal{E}_{\text{phase}}$ contains the terms of $\mathcal{E}$ which are diagonal in the computational basis, and $\mathcal{E}_{\text{other}}$ contains all other terms. Then, equations (1) and (2) remain unchanged if ε and ε' are re-interpreted as the norms of $\mathcal{E}_{\text{phase}}$ and $\mathcal{E}_{\text{other}}$, respectively. In the appendix, we give more details about this definition and about the derivation of the error rates that we discuss below.

Based on our modeling, we find the following hierarchy of expected error levels for the CPHASE gate: the rate for phase errors is 1.96×10^{-3} for qubit A and 4.6×10^{-3} for qubit B. For all other types of errors, the dominant contribution is due to *relaxation* to the ground state during the 35.1 ns duration of the CPHASE gate; using our previous results based on the Caldeira–Leggett model which give an estimate of $T_1 \approx 10$ ms [18, 23], we expect their rate to be around 3.5×10^{-6} for both qubits A and B. Therefore, as desired, there is a large contrast between the rates for phase errors and all other types of errors. We must also finally assess the magnitude of leakage. Since leakage errors cannot in general be corrected by our repetition code, it is crucial that leakage is suppressed to a very large extent; in fact, we have found that the rate for leakage errors is approximately 3.5×10^{-6}.

We have also designed pulses for the preparation of a qubit in the state $|+\rangle$, for single-qubit diagonal rotations, and for the measurement of σ_x; these pulses are only slightly modified from [18]. Since the diagonal rotations commute with the CPHASE gate, they can always be moved to occur immediately before the measurements of σ_x; the combined operation is a measurement of an operator of the form $\exp(\mathrm{i}\theta\sigma_z)\sigma_x$. The rate for phase errors in a preparation of $|+\rangle$ is 2.75×10^{-3} for both qubits A and B, and the rate for all other types of errors is 3.5×10^{-7}. However, because a preparation of $|+\rangle$ is performed by a *non-adiabatic* pulse, leakage is significantly larger than in the CPHASE gate; the leakage error rate is 3.77×10^{-7} for qubit A and 1.5×10^{-5} for qubit B. For a measurement of $\exp(\mathrm{i}\theta\sigma_z)\sigma_x$, we can describe noise in terms of effective errors of no specific structure preceding the ideal measurement, and their rate is 1.83×10^{-3} essentially independent of θ.

Given these physical-level error rates, we can obtain *upper bounds* on the error rates for the logical CNOT gate by using the equations in [19]. In this analysis, we use the error rates we have computed by averaging over a large number of simulations as fixed, constant error rates, and we will ignore any correlations between the fluctuations around these average values in space and time. The analysis must also consider leakage errors which are not discussed in [19]. Our method for analyzing leakage is based on the following observations. Firstly, as we have already noted, the fact that teleportation is used to implement the logical CNOT gate prevents leakage errors from propagating across multiple logical gates. In the worst case, one leakage error can propagate from the logical gate where it occurs to the following one. But this can be prevented by inserting a logical teleportation preceding every logical gate; i.e. the logical state of each output block from a logical gate is teleported to a new block as in figure 2 before the next logical gate is applied. Then, a leakage error that occurs in a logical gate or in the logical teleportations preceding it can only affect this logical gate and no other.

In our analysis of the logical CNOT gate, we have optimized over the block size n of the repetition code, and the number k of repetitions of measurements with ancilla qubits. For our physical-level error rates, the optimal choice is $(n, k) = (5, 7)$, where k is larger than n because qubits of species B (which are chosen as the ancilla qubits) are more noisy that qubits of species A (which are chosen as the data qubits). With this choice, we find that the logical CNOT gate has nearly balanced rates for phase errors and all other types of errors of at most 4.62×10^{-3} and 3.98×10^{-3}, respectively.

This is an improvement by a factor of about 3 over the best alternative method we have for implementing a CNOT gate without the encoding in the repetition code; as we have already discussed, we have found no direct implementation of a CNOT gate for the Koch qubit with an error rate better than 5%, and simulating the CNOT gate indirectly as in figure 1 leads to balanced rates for phase errors and all other types of errors of about 1.25%. Since our

error-rate upper bounds also apply to the other logical operations for the repetition code needed for universality [19], our analysis indicates that our estimated physical-level error rates for the Koch qubit are tantalizingly close to those needed for effective fault-tolerant operation; in the literature, the highest estimated error thresholds are of order 1%, and the best proven thresholds are of order 0.1% [15]–[17], [20].

To conclude, we have discussed an encoding scheme which has been especially tailored to the physical operations that are naturally available in the IBM qubit (CPHASE gates, qubit preparations and measurements), and the noise characteristics that can be expected for this system according to our theoretical modeling. We believe that the basic principles underlying our proposal—primarily, the implementation of *adiabatic* CPHASE gates with highly biased noise, and the suppression of phase errors by encoding in the repetition code—can be successfully adapted to apply to other promising systems besides flux qubits such as, e.g., superconducting phase qubits [4, 7].

Our estimated error rates incorporate contributions from all sources of noise which are understood in experiments at present. However, the experimental reality today is that noise is dominated by T_1 processes which are not fully understood, and coherence times are significantly below the values we have obtained from our calculation [18]. Our results should therefore be seen as preliminary and suggestive. Certainly, simplifications in modeling low-frequency $1/f$ noise have been made, so that noise fluctuations have been assumed to be constant during the execution of each gate, and also noise correlations and flux drifts across multiple gates have been ignored; see [18].

Furthermore, we should emphasize that there are several possibilities for complementing the methods of 'software' error correction we have described here with 'hardware' error correction which is done directly at the physical level; e.g. systematic noise correlations and flux drifts over long time scales could be suppressed by periodically recalibrating qubits off-line before they are re-used, or superconducting qubits could be designed to have physical error-correction properties as in [24] which uses the same set of elementary operations as ours. Finally, we should note that the topology of interactions for our repetition-code scheme is not attainable with short-range interactions on a square lattice. We expect however that a greater but limited range of interactions where each qubit is coupled to 10 or 20 other nearby qubits would suffice. Various possibilities exist for implementing such interactions for superconducting-qubit layouts where crossovers, multiple couplers and indirect couplings via transmission lines are all available.

Acknowledgments

DDV and BMT have been partly supported by IARPA under ARO contract no. W911NF-04-C-0098. JP is supported in part by DoE under grant no. DE-FG03-92-ER40701, NSF under grant no. PHY-0456720 and NSA under ARO contract no. W911NF-05-1-0294.

Appendix. Error rates

In our analysis, we model each noisy elementary operation by a superoperator. Therefore, we ignore temporal or spatial correlations between different operations, such as the correlations in time which are inevitably present for $1/f$ noise. We consider two sources of noise. First, $1/f$ noise in the control parameters—the applied fluxes, and the pulse synchronization—during the

execution of each operation; $1/f$ noise leads primarily to dephasing and it will be modeled by a superoperator $\mathcal{N}_{1/f}$. Secondly, thermal relaxation noise which is continuously present; relaxation is the primary source of errors other than phase errors and it will be modeled by an amplitude-damping superoperator $\mathcal{N}_{T_1}$.

Leakage errors depend both on the implementation of our operations and also on $1/f$ noise. We recall that during qubit preparation and measurement, which are implemented by *non-adiabatic* pulses, leakage can arise from Landau–Zener transitions to excited levels in the flux-qubit potential; during the execution of a CPHASE gate, leakage primarily occurs at the energy-level crossing marked C in figure 7(b). Since the relevant parameter is the minimum energy gap between states inside and outside the computational space during the implementation of an operation, leakage errors can occur even in the absence of $1/f$ noise. When $1/f$ noise is present, the minimum gaps are shifted from their ideal values when there is no noise, which in turn has an effect on leakage.

We model a noisy preparation of a qubit in the state $|+\rangle$ as the ideal preparation followed by the noise superoperator

$$\mathcal{N} \approx \mathcal{N}_{T_1} \circ \mathcal{N}_{1/f}, \tag{3}$$

where $\circ$ denotes composition. We model a noisy CPHASE gate as the ideal gate followed by a superoperator as in equation (3), where $\mathcal{N}_{1/f}$ is now supported on both qubits acted upon by the gate, and $\mathcal{N}_{T_1}$ is assumed to act independently on each of the two qubits. Finally, we model a noisy measurement of $\exp(\mathrm{i}\theta\sigma_z)\sigma_x$ as the ideal measurement *preceded* by a superoperator as in equation (3).

The noise superoperator for each elementary operation can be expressed in terms of a discrete set of Kraus operators (at most d^2 where d is the dimension of its support) [25]. If the identity is one of the Kraus operators, the noise model corresponds to local stochastic noise; in this case, we may define the phase error rate as the probability of all non-identity Kraus operators which are diagonal matrices in the computational basis. The probability of all other non-identity Kraus operators then defines the rate for all other types of errors. For this noise model, we can perform a fault-tolerance analysis to determine upper bounds on the probabilities of logical errors as in [19].

However, as we will discuss below, the superoperators in our modeling do not have this property so that noise cannot be simply described in terms of probabilistic errors. Nonetheless, we may use an alternative definition of an error rate, and with this definition the analysis in [19] remains essentially unchanged. The idea is to express $\mathcal{N}$ as the sum of an ideal and an erroneous part, $\mathcal{N} = \hat{\mathcal{I}} + \mathcal{E}$, where $\hat{\mathcal{I}}$ is a trace-decreasing superoperator which is proportional to the identity superoperator [26]. We may then define a generalized error rate or error *strength* in terms of the distance between $\mathcal{N}$ and $\hat{\mathcal{I}}$,

$$\varepsilon \equiv \|\mathcal{E}\|_\diamond = \|\mathcal{N} - \hat{\mathcal{I}}\|_\diamond, \tag{4}$$

where $\|\cdot\|_\diamond$ is the diamond norm [27]. If the superoperator $\mathcal{E}$ has an n-qubit input, $\|\mathcal{E}\|_\diamond = \|\mathcal{I}_n \otimes \mathcal{E}\|_1 = \max_{X:\|X\|_{\mathrm{tr}}=1} \|(\mathcal{I}_n \otimes \mathcal{E})(X)\|_{\mathrm{tr}}$, where $\mathcal{I}_n$ is the identity superoperator on n qubits, and $\|\cdot\|_{\mathrm{tr}}$ is the standard trace norm, i.e. $\|A\|_{\mathrm{tr}} = \mathrm{Tr}\sqrt{A^\dagger A}$.

In the remainder of this appendix, we give the details about the error rates for our elementary operations; the results are summarized in table 1. To simplify our calculations, we have estimated the various norms by only varying among a few possible inputs. Even though we have not performed a rigorous maximization, we believe that the inputs we have chosen are close to the worst case.

Table 1. Error-rate estimates for our elementary operations. For preparations and CPHASE gates, ε is the rate for phase errors, ε' is the rate for all other types of errors and ε_l is the rate for leakage errors. For measurements, the rate ε includes errors from all sources.

		Qubit A ($\omega_T = 2\pi \times 3.1$ GHz)		Qubit B ($\omega_T = 2\pi \times 3/4 \times 3.1$ GHz)
CPHASE	ε	1.96×10^{-3}		4.6×10^{-3}
	ε'	3.5×10^{-6}		3.5×10^{-6}
	ε_l		3.5×10^{-6}	
$\|+\rangle$ prep.	ε	2.75×10^{-3}		2.75×10^{-3}
	ε'	3.5×10^{-7}		3.5×10^{-7}
	ε_l	3.77×10^{-7}		1.5×10^{-5}
$\exp(i\theta\sigma_z)\sigma_x$ meas.	ε	1.83×10^{-3}		1.83×10^{-3}

$1/f$ *noise in* CPHASE *gates*

For the CPHASE gate, we have obtained the combined superoperator $\mathcal{N}_{1/f} \circ \mathcal{CZ}$ by integrating over the Gaussian fluctuations in the applied fluxes and the pulse timing as described in the main text; here, $\mathcal{CZ}$ is the ideal CPHASE superoperator (up to diagonal rotations on each qubit which are all moved before the measurements and will be discussed separately). From these numerical simulations, we can then extract the Kraus operators for $\mathcal{N}_{1/f}$. Each Kraus operator is supported on a 16-dimensional space $\mathcal{H}^{AB} = \mathcal{H}^A \otimes \mathcal{H}^B$, where $\mathcal{H}^A$ and $\mathcal{H}^B$ are 4-dimensional spaces corresponding to the two interacting Koch qubits A and B. For both qubits A and B,

$$\mathcal{H}^Q = \mathcal{H}^Q_{\text{flux}} \otimes \mathcal{H}^Q_{\text{trans}}, \tag{5}$$

where $\mathcal{H}^Q_{\text{flux}}$ is a 2-dimensional space spanned by the flux-qubit states $\{|L\rangle, |R\rangle\}$ and $\mathcal{H}^Q_{\text{trans}}$ is another 2-dimensional space spanned by the 0- and 1-photon states of the transmission line[9]. Since prior to and after the implementation of the CPHASE gate information is stored in the transmission-line modes, the computational space corresponds to the tensor product of the two transmission-line spaces, $\mathcal{H}^{AB}_{\text{trans}} = \mathcal{H}^A_{\text{trans}} \otimes \mathcal{H}^B_{\text{trans}}$; the action of the gate on the space $\mathcal{H}^{AB}_{\text{flux}} = \mathcal{H}^A_{\text{flux}} \otimes \mathcal{H}^B_{\text{flux}}$ is ideally trivial, and any transfer of amplitude to this space corresponds to leakage.

We have found that, within the precision of our numerical analysis[10], only four Kraus operators carry significant weight while all the rest are negligible. These four Kraus operators $\{M_0, \ldots, M_3\}$ are of the form

$$M_k = I_k + M_{k,d} + M_{k,\neg d} + M_{k,l}. \tag{6}$$

Here, I_k is proportional to the identity operator on $\mathcal{H}^{AB}$, $M_{k,d}$ includes all terms that act as the identity on $\mathcal{H}^{AB}_{\text{flux}}$ and as diagonal matrices in the computational basis on $\mathcal{H}^{AB}_{\text{trans}}$ (giving rise to phase errors), $M_{k,\neg d}$ contains all remaining terms acting as the identity on $\mathcal{H}^{AB}_{\text{flux}}$ (giving rise to

[9] Since transitions to states with more than one photon in a transmission line are negligible, in our numerical simulations we truncate the infinite-dimensional space of the transmission-line modes at the first excited state; see [18].

[10] We use 8 decimal digits of accuracy.

other types of errors in the computational basis), and finally $M_{k,l}$ includes all terms that act non-trivially on $\mathcal{H}^{AB}_{\rm flux}$ (giving rise to leakage errors).

If we expand in the Pauli basis in $\mathcal{H}^{AB}$, we find $\{I_0 = 0.9981\exp(\mathrm{i}1.2743) I^A \otimes I^B$, $I_1 = 0$, $I_2 = 0$, $I_3 = 0\}$,

$$\begin{aligned}
M_{0,d} &= 1.5\times10^{-4}\, I^A\otimes\sigma_z^B \quad +(1+3.5\mathrm{i})10^{-4}\,\sigma_z^A\otimes I^B \quad -(1.2+4.4\mathrm{i})10^{-4}\,\sigma_z^A\otimes\sigma_z^B,\\
M_{1,d} &= 5.2\times10^{-2}\, I^A\otimes\sigma_z^B \quad +9\times10^{-3}\,\sigma_z^A\otimes I^B \quad -7\times10^{-3}\,\sigma_z^A\otimes\sigma_z^B,\\
M_{2,d} &= 1.8\times10^{-3}\, I^A\otimes\sigma_z^B \quad +1\times10^{-2}\,\sigma_z^A\otimes I^B \quad +4.6\times10^{-4}\,\sigma_z^A\otimes\sigma_z^B,\\
M_{3,d} &= 1\times10^{-4}\, I^A\otimes\sigma_z^B \quad +(7.4-\mathrm{i})10^{-4}\,\sigma_z^A\otimes\sigma_z^B,
\end{aligned} \tag{7}$$

where $I^A = I^B = I\otimes I$ and $\sigma_z^A = \sigma_z^B = I\otimes\sigma_z$ according to the tensor-product structure in equation (5). For brevity, we will omit the expressions for $\{M_{k,\neg d}\}$ and $\{M_{k,l}\}$.

We may write $\mathcal{N}_{1/.f} = \hat{\mathcal{I}} + \mathcal{E}_l + \mathcal{E}_{\neg d} + \mathcal{E}_d$, where $\hat{\mathcal{I}}(X) = \sum_{k=0}^{3} I_k X I_k^\dagger$ is trace-decreasing and proportional to the identity superoperator, $\mathcal{E}_l$ contains all terms with at least one insertion of a leakage error $\{M_{k,l}\}$, i.e.,

$$\mathcal{E}_l(X) = \mathcal{N}_{1/f}(X) - \sum_{k=0}^{3}(I_k + M_{k,d} + M_{k,\neg d})X(I_k + M_{k,d} + M_{k,\neg d})^\dagger, \tag{8}$$

$\mathcal{E}_{\neg d}$ contains all remaining terms with at least one insertion of a non-dephasing error $\{M_{k,\neg d}\}$, i.e.,

$$\mathcal{E}_{\neg d}(X) = (\mathcal{N}_{1/f} - \mathcal{E}_l)(X) - \sum_{k=0}^{3}(I_k + M_{k,d})X(I_k + M_{k,d})^\dagger, \tag{9}$$

and $\mathcal{E}_d$ contains all remaining terms with at least one insertion of a phase error $\{M_{k,d}\}$, i.e.,

$$\mathcal{E}_d(X) = (\mathcal{N}_{1/f} - \mathcal{E}_l - \mathcal{E}_{\neg d})(X) - \sum_{k=0}^{3} I_k X I_k^\dagger. \tag{10}$$

We define the rate of leakage errors as the norm of $\mathcal{E}_l$; by taking as the worst-case input the state $|\tilde{1}\rangle|\tilde{1}\rangle$ (cf figure 7(b)), we find $\|\mathcal{E}_l\|_\diamond \approx 3.5\times10^{-6}$. Similarly, we define the rate of non-dephasing errors as the norm of $\mathcal{E}_{\neg d}$; we find $\|\mathcal{E}_{\neg d}\|_\diamond = O(10^{-7})$, which can be neglected since it is much smaller than the contribution due to relaxation to be discussed below.

We finally define the rate for phase errors as the norm of $\mathcal{E}_d$. By varying among several possible inputs, we obtained the largest value of $\|\mathcal{E}_d\|_\diamond \approx 4.73\times10^{-3}$ for the Bell state

$$|\Phi_0\rangle = \frac{1}{\sqrt{2}}(|\tilde{0}\rangle|\tilde{0}\rangle + |\tilde{1}\rangle|\tilde{1}\rangle). \tag{11}$$

Here, $|\tilde{0}\rangle \equiv |S\rangle|0_p\rangle$ and $|\tilde{1}\rangle \equiv |S\rangle|1_p\rangle$, where $|S\rangle = \frac{1}{\sqrt{2}}(|L\rangle + |R\rangle)$ is the symmetric state in $\mathcal{H}^Q_{\rm flux}$ and $|n_p\rangle$ is the n-photon state in $\mathcal{H}^Q_{\rm trans}$ with Q either A or B; see figures 6 and 7.

We may also estimate the rates for phase errors on qubit A and qubit B separately. For qubit A, we modify our expansion by writing $\mathcal{N}_{1/f} = \hat{\mathcal{I}}^A + \mathcal{E}_l + \mathcal{E}_{\neg d} + \mathcal{E}_d^A$, where

$$\hat{\mathcal{I}}^A(X) = \sum_{k=0}^{3}(I_k + M_{k,d}^B)X(I_k + M_{k,d}^B)^\dagger, \tag{12}$$

and $M^B_{k,d}$ includes those terms in $M_{k,d}$ which are proportional to $I^A \otimes \sigma_z^B$ and so act trivially on qubit A. Then, $\mathcal{E}^A_d$ captures all terms that apply nontrivial phase noise to qubit A. By using the same Bell state as input, we find that phase errors on qubit A have a rate $\|\mathcal{E}^A_d\|_\diamond \approx 1.96 \times 10^{-3}$. If we perform a similar analysis for qubit B instead, we find $\|\mathcal{E}^B_d\|_\diamond \approx 4.6 \times 10^{-3}$. This shows that the effect of $1/f$ noise on qubit B is stronger than on qubit A, which is physically expected since qubit A is unparked much less deeply than qubit B during the implementation of a CPHASE gate; see figure 7.

$1/f$ *noise in preparation*

For the preparation of the state $|+\rangle$, we have obtained the density matrix $\rho_{|+\rangle} = \mathcal{N}_{1/f}(|+\rangle\langle+|)$ by performing a similar integration over the fluctuating fields as for the CPHASE gate. Depending on the species of qubit, $\rho_{|+\rangle}$ is supported on $\mathcal{H}^Q$ for Q either A or B, and it is of the form

$$\rho_{|+\rangle} = \eta_{|+\rangle,d} + \eta_{|+\rangle,l}; \tag{13}$$

here, $\eta_{|+\rangle,d}$ is an operator supported on $|S\rangle\langle S| \otimes \mathcal{H}^Q_{\text{trans}}$, and $\eta_{|+\rangle,l}$ includes all remaining terms of $\rho_{|+\rangle}$. Since after the preparation the information is stored in the transmission-line modes, the ideal state is $|\tilde{+}\rangle\langle\tilde{+}| = |S\rangle\langle S| \otimes |+_p\rangle\langle+_p|$ from which we can obtain $\eta_{|+\rangle,d}$ by acting with phase errors alone; on the other hand, for all terms in $\eta_{|+\rangle,l}$ the state of the flux qubit is orthogonal to $|S\rangle$ so that leakage has occurred.

We define the rate of leakage errors as $\varepsilon_l = \|\eta_{|+\rangle,l}\|_{\text{tr}}$; for qubit A we find $\varepsilon_l \approx 3.77 \times 10^{-7}$, while for qubit B we find $\varepsilon_l \approx 1.5 \times 10^{-5}$ (our pulses are not highly optimized to avoid leakage, and we believe the leakage error rate for qubit B can be improved if necessary). For phase errors, we define the rate as $\varepsilon = \|\eta_{|+\rangle,d} - c|\tilde{+}\rangle\langle\tilde{+}|\|_{\text{tr}}$ where we are allowed to optimize over the choice of $0 \leqslant c \leqslant 1$; for both qubits A and B, we find $\varepsilon \approx 2.75 \times 10^{-3}$.

$1/f$ *noise in measurement*

A measurement of $\exp(\mathrm{i}\theta\sigma_z)\sigma_x$ is implemented by applying the diagonal rotation $\exp(-\mathrm{i}\theta\sigma_z)$ on $\mathcal{H}^Q_{\text{trans}}$, followed by a non-adiabatic pulse mapping $|\tilde{+}\rangle$ and $|\tilde{-}\rangle$ (where information is stored in the transmission-line modes) to $|0\rangle \equiv |L\rangle|0_p\rangle$ and $|1\rangle \equiv |R\rangle|0_p\rangle$ respectively (where information is stored in the flux-qubit states), followed by a projection along the basis $\{|L\rangle, |R\rangle\}$.

Diagonal rotations can be executed with pulses of short duration so that errors are very weak compared to other operations and can be neglected. We also assume that errors during the final projection can be neglected. The states $|L\rangle$ and $|R\rangle$ can be distinguished very accurately by setting Φ_C very small ($\sim 1.4\Phi_0$) so that there is a large potential barrier between them resulting in very high T_1 in the $\{|L\rangle, |R\rangle\}$ basis (cf figure 6); since the two states correspond to distinct circulating-current orientations, they induce different magnetic signals which can be detected by using the SQUIDs (cf figure 5).

To obtain the error rate for the remaining measurement process, we follow the evolution of the basis states $|\tilde{+}\rangle$ and $|\tilde{-}\rangle$ by performing a numerical simulation similar to the cases already discussed. If the initial state is $|\tilde{+}\rangle$, we calculate the probability that the final state before the projection is orthogonal to $|0\rangle$, in which case we assume an error in the measurement outcome always occurs; and similarly for $|\tilde{-}\rangle$, we calculate the probability that the final state is orthogonal to $|1\rangle$. We define this probability as the error rate for the measurement; for both qubits A and B, we find $\varepsilon \approx 1.83 \times 10^{-3}$.

Relaxation

We model relaxation noise by the amplitude-damping superoperator $\mathcal{N}_{T_1}$ acting independently on each qubit; with Q either A or B, the two Kraus operators are

$$M_0 = \frac{1+\sqrt{1-\gamma}}{2} I^Q + \frac{1-\sqrt{1-\gamma}}{2} \sigma_z^Q, \quad M_1 = \frac{\sqrt{\gamma}}{2} \sigma_x^Q (1-\sigma_z^Q), \tag{14}$$

where we have already defined I^Q and σ_z^Q, and $\sigma_x^Q = I \otimes \sigma_x$ according to the tensor-product structure in equation (5).

Since only M_1 is non-diagonal in the computational basis, we define the rate for non-dephasing errors as $\|\mathcal{M}_1\|_\diamond = \gamma$, where $\mathcal{M}_1(X) = M_1 X M_1^\dagger$. We also define the rate for phase errors due to the operator M_0 as $\|\mathcal{M}_0 - \hat{\mathcal{I}}\|_\diamond$, where $\mathcal{M}_0(X) = M_0 X M_0^\dagger$ and $\hat{\mathcal{I}}(X) = cX$ with $0 \leqslant c \leqslant 1$. If we take $c = \left(1+\sqrt{1-\gamma}\right)^2/4$, we find $\|\mathcal{M}_0 - \hat{\mathcal{I}}\|_\diamond \approx \gamma/2$.

For a CPHASE gate, we use the worst-case estimate $T_1 = 10\,\text{ms}$, and we assume T_1 can be treated as approximately constant during the execution of the gate; then, $\gamma = t/T_1 = 3.5 \times 10^{-6}$ where $t = 35\,\text{ns}$ is the duration of the gate. For diagonal rotations which are executed with pulses of duration $t \leqslant 5\,\text{ns}$, γ is very small and can be neglected. Finally, for preparation and measurement, T_1 changes as a function of the control flux and we calculate $\gamma = \int_0^t \mathrm{d}s \frac{s}{T_1(s)} = 3.5 \times 10^{-7}$.

References

[1] You J Q and Nori F 2005 Superconducting circuits and quantum information *Phys. Today* **58** 42–7

[2] Nakamura Y, Pashkin Yu A and Tsai J S 1999 Coherent control of macroscopic quantum states in a single-Cooper-pair box *Nature* **398** 786–8

[3] Vion D *et al* 2002 Manipulating the quantum state of an electrical circuit *Science* **296** 886–9

[4] Martinis J M, Nam S, Aumentado J and Urbina C 2002 Rabi oscillations in a large Josephson-junction qubit *Phys. Rev. Lett.* **89** 117901

[5] Chiorescu I, Nakamura Y, Harmans C J P M and Mooij J E 2003 Coherent quantum dynamics of a superconducting flux qubit *Science* **299** 1869–71

[6] Wallraff A *et al* 2004 Strong coupling of a single photon to a superconducting qubit using circuit quantum electrodynamics *Nature* **431** 162–7

[7] Steffen M *et al* 2006 Measurement of the entanglement of two superconducting qubits via state tomography *Science* **313** 1423–5

[8] Koch R H *et al* 2006 Experimental observation of an oscillator-stabilized Josephson qubit *Phys. Rev. Lett.* **96** 127001

[9] Aharonov D and Ben-Or M 1997 Fault-tolerant quantum computation with constant error *Proc. 29th Annual ACM Symp. on the Theory of Computation* (New York: ACM) pp 176–88 (arXiv:quant-ph/9611025)

[10] Knill E, Laflamme R and Zurek W 1998 Resilient quantum computation: error models and thresholds *Proc. R. Soc. Lond.* A **454** 365–84 (arXiv:quant-ph/9702058)

[11] Preskill J 1998 Fault-tolerant quantum computation *Introduction to Quantum Computation* ed H-K Lo, S Popescu and T P Spiller (Singapore: World Scientific) pp 213–69 (arXiv:quant-ph/9712048)

[12] Kerman A J and Oliver W D 2008 High-fidelity quantum operations on superconducting qubits in the presence of noise *Phys. Rev. Lett.* **101** 070501

[13] Montangero S, Calarco T and Fazio R 2007 Robust optimal quantum gates for Josephson charge qubits *Phys. Rev. Lett.* **99** 170501

[14] Koch R H *et al* 2005 Low-bandwidth control scheme for an oscillator-stabilized Josephson qubit *Phys. Rev.* B **72** 092512

[15] Knill E 2005 Quantum computing with realistically noisy devices *Nature* **434** 39–44 (arXiv:quant-ph/0410199)
[16] Aliferis P, Gottesman D and Preskill J 2008 Accuracy threshold for postselected quantum computation *Quantum Inf. Comput.* **8** 181 (arXiv:quant-ph/0703264)
[17] Raussendorf R and Harrington J 2007 Fault-tolerant quantum computation with high threshold in two dimensions *Phys. Rev. Lett.* **98** 190504 (arXiv:quant-ph/0610082)
[18] Brito F, DiVincenzo D P, Koch R H and Steffen M 2008 Efficient one- and two-qubit pulsed gates for an oscillator-stabilized Josephson qubit *New J. Phys.* **10** 033027 (arXiv:0709.1478)
[19] Aliferis P and Preskill J 2008 Fault-tolerant quantum computation against biased noise *Phys. Rev.* A **78** 052331 (arXiv:0710.1301)
[20] Cross A W, DiVincenzo D P and Terhal B M 2007 A comparative code study for quantum fault-tolerance arXiv:0711.1556
[21] Aliferis P and Terhal B M 2007 Fault-tolerant quantum computation for local leakage faults *Quantum Inf. Comput.* **7** 139–57 (arXiv:quant-ph/0511065)
[22] Koch R H and Steffen M unpublished
[23] DiVincenzo D P, Brito F and Koch R H 2006 Efficient evaluation of decoherence rates in complex Josephson circuits *Phys. Rev.* B **74** 014514
[24] Kitaev A 2006 Protected qubit based on a superconducting current mirror arXiv:cond-mat/0609441
[25] Preskill J e.g. see *Lecture Notes of Quantum Computation Course* chapter 3 available at http://www.theory.caltech.edu/people/preskill/ph229/#lecture
[26] Aharonov D and Ben-Or M 1999 Fault-tolerant quantum computation with constant error rate arXiv:quant-ph/9906129
[27] Kitaev A Yu, Shen A H and Vyalyi M N 2002 *Classical and Quantum Computation* (*Graduate Studies in Mathematics* vol 47) (Providence, RI: American Mathematical Society)